

---

# Language Model Distillation: A Temporal Difference Imitation Learning Perspective

---

**Zishun Yu\***

Department of Computer Science  
The University of Illinois, Chicago  
Chicago, IL 60607  
zyu32@uic.edu

**Shangzhe Li\***

Department of Computer Science  
The University of North Carolina at Chapel Hill  
Chapel Hill, NC 27599  
shangzhe@unc.edu

**Xinhua Zhang**

Department of Computer Science  
The University of Illinois, Chicago  
Chicago, IL 60607  
zhangx@uic.edu

## Abstract

Large language models have led to significant progress across many NLP tasks, although their massive sizes often incur substantial computational costs. Distillation has become a common practice to compress these large and highly capable models into smaller, more efficient ones. Many existing language model distillation methods can be viewed as behavior cloning from the perspective of imitation learning or inverse reinforcement learning. This viewpoint has inspired subsequent studies that leverage (inverse) reinforcement learning techniques, including variations of behavior cloning and temporal difference learning methods. Rather than proposing yet another specific temporal difference method, we introduce a general framework for temporal difference-based distillation by exploiting the distributional sparsity of the teacher model. Specifically, it is often observed that language models assign most probability mass to a small subset of tokens. Motivated by this observation, we design a temporal difference learning framework that operates on a reduced action space (a subset of vocabulary), and demonstrate how practical algorithms can be derived and the resulting performance improvements.

## 1 Introduction

The successes of large language models (LLMs) have brought transformative advancements across many NLP tasks, albeit often at the cost of substantial computational resources due to their massive size. Model distillation is a widely adopted approach to compressing these large, high-capacity models (teachers) into smaller, efficient models (students). This practice has become standard, ranging from proprietary ones [1] to open-source model families [2–6].

The seminal work of knowledge distillation (KD) proposed by Hinton et al. [7] established the foundation for distribution-matching distillation methods, which were later extended to sequence/autoregressive models [8]. In distribution-matching methods, at each time step during text generation, a student model  $\pi : \mathcal{X} \rightarrow \Delta(\mathcal{V})$  seeks to approximate the probability distribution, over an vocabulary  $\mathcal{V}$ , produced by the teacher  $\pi^*$ , for example by minimizing a (forward) KL-divergence [9–11]

---

\*Equal contributions.

$\min_{\pi} \mathbb{KL}[\pi^*(x_{\leq t}) || \pi(x_{\leq t})]$ , where  $x_{\leq t} \in \mathcal{X}$  is a sequence of length  $t$ , and  $\Delta(\Omega)$  denotes a probability simplex over space  $\Omega$ .

Notably, this sequential distribution matching can be interpreted as behavior cloning (BC) [12], within the imitation learning (IL) and inverse reinforcement learning (IRL) literature [13–17]. While there are nuanced differences between IL and IRL, we use them interchangeably.

An important distinction between IL and distillation lies in the accessibility of the expert/teacher model  $\pi^*$ . In IL settings,  $\pi^*$  is typically not available as a white-box model; instead, it is inferred empirically from expert demonstrations. A common estimate is given by  $\hat{\pi}^*(y | x) \propto \mathbb{E}_{(s,a) \sim \rho_{\mathbb{D}}} [\mathbb{1}_{\{(x,y)=(s,a)\}}]$ , where  $\rho_{\mathbb{D}}$  is the empirical distribution induced from a dataset  $\mathbb{D}$ . In contrast, it is reasonable to assume direct access to  $\pi^*$  as a white-box for distillation. This suggests that distillation is an even easier problem to IL, enabling the application of tools and insights from the broader IL literature.

Casting distillation as an IL problem is not new per se; indeed, many existing distillation works [8, 18–20] perform BC. Before reviewing these works through the lens of IL, we highlight two key distinctions that help characterize the distillation setup: (i) offline vs. online: This refers to whether distillation is performed on a fixed, pre-collected dataset (offline) or involves continuously generating new data during training (online). (ii) off-policy vs. mixed-policy: A method is considered purely on-policy if it uses only student-generated data for training; otherwise, it is categorized as off-policy. However, purely on-policy distillation is rare in practice—most methods use a mixture of teacher and student data. We refer to this setup as mixed-policy, though it is technically off-policy in the RL literature.

The pioneer work of sequence-level KD (SeqKD) [8] is an offline off-policy BC. Follow up BC style works fall into two main categories: (i) online mixed-policy [18, 19, 21]; and (ii) offline mixed-policy [20]; potentially with different choice of divergence measure - forward/reverse KL [8, 19], Jensen-Shannon divergence [18], and general  $f$ -divergence [20].

However, BC is known to suffer from compounding errors [22, 23], also referred as exposure bias [24] in the context of auto-regressive models. To address these issues, the IL literature offers a rich toolbox beyond BC, for example generative adversarial training [17], occupancy matching [25], and more. We refer readers to Osa et al. [26] for a comprehensive review. While not exhaustive, many modern IL methods [25, 17, 16] involve modeling an inverse reward function and then optimizing a policy with respect to it using RL. These RL algorithms are often based on temporal-difference (TD) learning [27], which estimates the long-term impact of an action (or token) given a state (or sub-sequence) to mitigate the compounding errors.

Distillation may potentially benefit from the broader IL toolbox—particularly from TD learning methods. Earlier work has already demonstrated the potential of such approaches in smaller auto-regressive models. For instance, Yu et al. [28] and Wu et al. [29] can be viewed as early applications of Ho and Ermon [17]. For modern LLMs, Jia [30] explored TD-style IL methods for distillation, through value moment matching [13, 16, 31] in particular. However, applying TD learning to LLMs is generally challenging due to their vast state-action space  $\mathcal{V}^T$  [32–34].

Instead of directly applying a specific TD-learning-based IL method to distillation, we ask a more fundamental question: is there an exploitable structure unique to the distillation setting? A natural observation is that, for LLMs, the output distribution over the vocabulary is often sparse—only a small subset of tokens typically receive significant probability mass. An illustrative example is shown in Figure 1: For responses we generated, top 50 tokens account for 96% total mass, and top 7 tokens contribute 90%. Motivated by this observation, a natural idea is: during TD learning, it may be

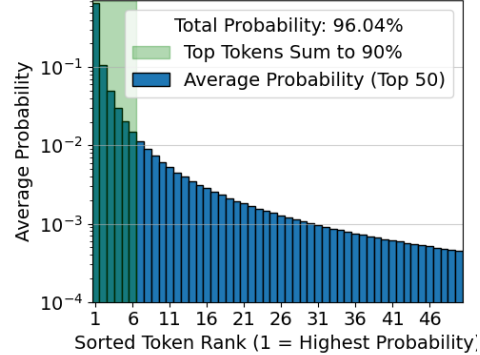


Figure 1: We average the sorted token probabilities across 20 sequences generated by Qwen-2.5 3B. Top 50 tokens account for 96% of the total mass, and the top 7 tokens contribute  $\geq 90\%$ .

sufficient to consider only a small subset of candidate actions, reducing the effective action space from  $\mathcal{V}$  to a much smaller set.

## 2 Preliminaries

**MDP notations.** We define the conventional MDP tuple  $\mathcal{M} = (\mathcal{S}, \mathcal{A}, \mathcal{T}, r, \gamma)$  as follows. Let  $w_{\leq t} = (w_1, w_2, \dots, w_t) \in \mathcal{W}_t := \mathcal{V}^t$  be a sequence of tokens. We define a state and an action as  $s_t := s_0 \circ w_{\leq t} \in \mathcal{S}$  and  $a_t := w_t \in \mathcal{A}$ , where  $\circ$  denotes concatenation and  $s_0$  is a prompt (or a query). We will sometimes use  $x$  and  $y$  as substitute of  $s$  and  $a$  whenever required by context, and use the conventional prime notation  $s', a'$  to denote  $s_{t+1}, a_{t+1}$  when only relative temporal index matters. The transition function  $\mathcal{P} : \mathcal{S} \times \mathcal{A} \rightarrow \mathcal{S}$  is defined as simple concatenation  $s' = \mathcal{P}(s, a) := s \circ a$ ;  $r : \mathcal{S} \times \mathcal{A} \rightarrow \mathbb{R}$  is an unknown reward function; and  $\gamma \in [0, 1]$  is a discount factor.

**Policy.** We denote the student policy as  $\pi : \mathcal{S} \rightarrow \Delta(\mathcal{A})$  (or parameterized  $\pi_\theta$ ) and the teacher model as  $\pi^* : \mathcal{S} \rightarrow \Delta(\mathcal{A})$ , which may sometimes be referred to as the expert policy using IL terminology.

**Soft value functions.** The goal of soft RL is to maximize the expected return  $J(\pi) = \mathbb{E}[\sum_t \gamma^t \tilde{r}_t \mid \pi, \mathcal{M}]$ . The state-action value function  $Q^\pi : \mathcal{S} \times \mathcal{A} \rightarrow \mathbb{R}$  and the state value function  $V^\pi : \mathcal{S} \rightarrow \mathbb{R}$  are essentially recursive definition of the return  $J(\pi)$ . In particular, we consider soft value functions (entropy-regularized) [35, 16] in this work, which are defined as follows:

$$Q^\pi(s, a) := \mathbb{E}[\sum_{t=0}^{\infty} \gamma^t \tilde{r}_t \mid \pi, \mathcal{M}, S_0 = s, A_0 = a] = r(s, a) + \gamma V^\pi(s'), \quad (1)$$

$$V^\pi(s) := \mathbb{E}_{a \sim \pi(s)}[Q(s, a) - \log \pi(a \mid s)] \quad (2)$$

where  $s' = s \circ a$ , and  $\tilde{r}(s, a) := r(s, a) - \log \pi(a \mid s)$  is the entropy-regularized reward.

In an operator notation, the soft Bellman operator  $\mathcal{B}_r^\pi : \mathbb{R}^{\mathcal{S} \times \mathcal{A}} \rightarrow \mathbb{R}^{\mathcal{S} \times \mathcal{A}}$  is defined as  $(\mathcal{B}_r^\pi Q)(s, a) = r(s, a) + \gamma V^\pi(s')$ . Note this soft Bellman (evaluation) operator is a contractor [36], in contrast to the non-contractive soft Bellman improvement operator [35]. We will throughout this paper use soft Bellman operator to denote  $\mathcal{B}_r^\pi$ , the policy evaluation operator.

**Remark on  $\mathcal{B}_r^\pi$ .** The contractive property of  $\mathcal{B}_r^\pi$  defines a unique soft  $Q$ -function, for a reward function  $r$ , as the fixed point of  $Q = \mathcal{B}_r^\pi Q$ , given the Banach fixed-point theorem [37]. The contraction property of  $\mathcal{B}_r^\pi$  later helps us to obtain our results in Section 3.

**Occupancy measures.** Let  $x$  be a state, the occupancy measure induced from a policy  $\pi$  is  $\rho_x^\pi(s, a) := \mathbb{E}_\pi[\sum_{t=\tau}^{\infty} \gamma^{t-\tau} \mathbb{1}_{\{S_t=s, A_t=a\}} \mid S_\tau = x]$ . Occupancy measures are convenient notation for formulating RL problems, though not a must, we introduce them to make the formulations more succinct. It is convenient as the value function can be written as  $V^\pi(s) = \mathbb{E}_{(x,y) \sim \rho_s^\pi}[\tilde{r}(x, y)]$ .

**Max-entropy IRL.** With these definitions, we are now ready to introduce our choice of concrete IRL algorithm, IQL [38], which is an extension of maximum-entropy IRL [16]. We start with the Generative Adversarial IL (GAIL) [17] objective function:

$$\min_{\pi} \max_r L(\pi, r) := \mathbb{E}_{\rho^*}[r(s, a)] - \mathbb{E}_{\rho^\pi}[r(s, a)] - \mathcal{H}(\pi) - \psi(r), \quad (3)$$

where  $\mathcal{H}(\pi) := \mathbb{E}_{\rho^\pi}[-\log \pi(a \mid s)]$  and  $\psi : \mathbb{R}^{\mathcal{S} \times \mathcal{A}} \rightarrow \mathbb{R}$  is a convex reward regularizer.

**Inverse soft Q-learning.** IQL [38] is a recent popular extension of GAIL, which is also the choice of algorithm of our paper. It's objective function is defined as:

$$\max_Q \min_{\pi} \mathcal{J}(\pi, Q) := \mathbb{E}_{\rho^*}[Q(s, a) - \gamma V^\pi(s')] - (1 - \gamma) \mathbb{E}_{s_0}[V^\pi(s_0)] - \psi(\mathcal{T}^\pi Q), \quad (4)$$

$$\Leftrightarrow \max_Q \mathcal{J}^*(Q) := \mathbb{E}_{\rho^*}[\phi(Q(s, a) - \gamma V^Q(s'))] - (1 - \gamma) \mathbb{E}_{s_0}[V^Q(s_0)] \quad (5)$$

where  $\phi$  is a choice of concave regularizer;  $\mathcal{T}^\pi : \mathbb{R}^{\mathcal{S} \times \mathcal{A}} \rightarrow \mathbb{R}^{\mathcal{S} \times \mathcal{A}}$  is an inverse soft Bellman operator, defined as  $(\mathcal{T}^\pi Q)(s, a) = Q(s, a) - \gamma V^\pi(s')$ ; and  $V^Q := \log \sum_a \exp Q(s, a)$ .

The core idea is can be summarized as: (i) The original GAIL objective  $\min_{\pi} \max_r L(\pi, r)$  can be equivalently swapped as  $\max_r \min_{\pi} L(\pi, r)$  by strong duality, given proper regularization and feasible domains; (ii) For a fixed policy  $\pi$ , the saddle-point problem  $\max_r \min_{\pi} L(\pi, r)$  for a fixed  $\pi$  is provably equivalent to  $\max_Q \min_{\pi} \mathcal{J}(\pi, Q)$ . This equivalence allows direct optimization in the value-function space, eliminating the need to explicitly model the inverse reward  $r$ ; (iii) For a fixed  $Q$ , it is well-known that the entropy-regularized policy has a closed-form solution given

by  $\pi_Q = \exp Q(s, a) / \sum_a \exp Q(s, a)$ . And Danskin’s theorem [39] implies the saddle-point optimization  $\max_Q \min_\pi \mathcal{J}(\pi, Q)$  can be casted as a simple maximization  $\max_Q \mathcal{J}^*(Q)$ .

**Remark on IQL.** IQL reparameterizes the saddle-point formulation of IRL, enabling simpler and more stable optimization, and has thus recently gained popularity. We refer readers to [17, 38, 40], for a detailed derivation, background, and follow-up works. Throughout this paper, we use the deterministic form of IQL since the transition function  $\mathcal{P}$  for LLMs is deterministic; the original stochastic formulation can be found in Garg et al. [38].

### 3 Method

#### 3.1 Notation Setup

Defining different sort of backup operators with different desired properties has been a significant string of works in the RL literature. We refer to Asadi and Littman [41] and Miahhi et al. [42] for detailed discussions. We start with the example of soft Bellman operator used in IQL

$$(\mathcal{B}_r^\pi Q)(s, a) = r(s, a) + \gamma \mathbb{E}_{a' \sim \pi(s')} [Q(s', a') - \log \pi(a' | s')]] \quad (6)$$

The future term  $\mathbb{E}_{a' \sim \pi(s')} [Q(s', a') - \log \pi(a' | s')]$  is often called target. While evaluating the target, the candidate set of actions is the entire action space  $\mathcal{A} = \mathcal{V}$ , which is often huge.

Given the sparsity observation we made in Figure 1, a natural idea is to only use a subset of candidate actions that have a significant total density mass, say top- $p$  tokens, we define the top- $p$  candidate set:

**Definition 1** (top- $p$  candidate set). *Given  $\pi^*$  and a state  $s$ , the top- $p$  candidate set is defined as*

$$\mathcal{A}_p^*(s) := \{a_i : \sum_i \pi^*(a_i | s) = p; \pi^*(a_i | s) \geq \pi^*(a_j | s) \forall i, j\} \subseteq \mathcal{A}. \quad (7)$$

where actions are sorted in descending order of probability density (i.e.,  $\pi^*(a_i | s) \geq \pi^*(a_j | s)$  for all  $i < j$ ). Thus, for state  $s$ , the set  $\mathcal{A}_p^*(s)$  consists of actions with the largest probabilities whose cumulative probability equals  $p$ , a.k.a. top- $p$  tokens [43]. Although it’s uncommon to have a set whose cumulative probability equals exactly  $p$ , we use this notation for brevity, as the intended meaning is clear from context.

This top- $p$  set filtered out the actions that have low densities w.r.t. the teacher  $\pi^*$ . It is intuitive as the teacher model is a high-capable model and hence the reserved candidate tokens are high-quality.

**Remark on  $\mathcal{A}_p^*(s)$ .** Note that  $\mathcal{A}_p^*(s)$  is a state-dependent set, which creates notational inconvenience for subsequent analysis. Without loss of generality, we simplify that  $\mathcal{A}_p^*$  is state-independent, it is easy to extend the following results to state-dependent  $\mathcal{A}_p^*(s)$ . A simple construction is  $\mathcal{A}_p^* := \cup_s \mathcal{A}_p^*(s)$ .

Instead proceeding to direct implementation with this top- $p$  set, lets first define a top- $p$  MDP  $\mathcal{M}_p$  as a filtered counterpart of the original MDP  $\mathcal{M}$ .

**Definition 2** (top- $p$  MDP and  $\bar{Q}$ ). *Given a MDP  $\mathcal{M} = (\mathcal{S}, \mathcal{A}, \mathbb{P}, r, \gamma)$  and a teacher policy  $\pi^*$ , its top- $p$  counterpart is  $\mathcal{M}_p = (\mathcal{S}, \mathcal{A}_p^*, \mathbb{P}, r, \gamma)$ . To make the notation clearer, we use  $Q : \mathcal{S} \times \mathcal{A} \rightarrow \mathbb{R}$  and  $\bar{Q} : \mathcal{S} \times \mathcal{A}_p^* \rightarrow \mathbb{R}$  to denote  $Q$ -functions live in  $\mathcal{M}$  and  $\mathcal{M}_p$ , respectively.*

With this definition, we aim to address an important question: **What’s the performance of the optimal policy, if exist any, in  $\mathcal{M}_p$  compared to the optimal policy in  $\mathcal{M}$ ? Do we preserve proximal optimality when we use a subset of actions  $\mathcal{A}_p^*$ ?**

Let  $\pi^*$  and  $Q^*$  be the optimal policy and its corresponding soft  $Q$ -function in  $\mathcal{M}$ , and let  $\pi_p^*$  and  $\bar{Q}_p^*$  denote their counterpart in  $\mathcal{M}_p$ . As  $\mathcal{M}_p$  is also a well-defined MDP, the existence of  $\pi^*$ ,  $\pi_p^*$ ,  $Q^*$ ,  $\bar{Q}_p^*$  follows directly from the fixed point theorem [37]. Note that we use  $\pi^*$  to refer to both optimal policy and the teacher model, as in IRL it is often assumed that the demonstrator (the teacher) is optimal.

**Definition 3** (top- $p$  projection). *For any policy  $\pi$ , its top- $p$  counterpart in the top- $p$  MDP  $\mathcal{M}_p$  is a state-wise projection  $\text{PROJ}_p$  onto the top- $p$  candidate set  $\mathcal{A}_p^*$ , for all state  $s \in \mathcal{S}$ .*

$$\text{PROJ}_p(\pi)(a | s) := \begin{cases} \pi(a | s) / \sum_{a \in \mathcal{A}_p^*} \pi(a | s), & \text{if } a \in \mathcal{A}_p^* \\ 0, & \text{otherwise} \end{cases} \quad (8)$$

**Remark on  $\text{PROJ}_p$ .**  $\text{PROJ}_p(\pi_p^*) = \pi_p^*$  by definition, and  $\text{PROJ}_p(\pi^*)$  is not necessarily  $\pi_p^*$ . However, the projected policy  $\text{PROJ}_p(\pi^*)$  is handy for our analysis, see later Proposition 3 and 4.

With this projection definition, we are now ready to define a top- $p$  version of soft Bellman operator.

**Definition 4** (top- $p$  soft Bellman operator). *For any policy  $\pi : \mathcal{S} \times \mathcal{A} \rightarrow \Delta(\mathcal{A})$  and reward function  $r$ , We define a top- $p$  counterpart  $\mathcal{B}_p^\pi : \mathbb{R}^{\mathcal{S} \times \mathcal{A}_p^*} \rightarrow \mathbb{R}^{\mathcal{S} \times \mathcal{A}_p^*}$  to the soft Bellman operator  $\mathcal{B}_r^\pi$  as*

$$(\mathcal{B}_p^\pi \bar{Q})(s, a) = r(s, a) + \gamma \mathbb{E}_{a' \sim \text{PROJ}_p(\pi)}[\bar{Q}(s', a') - \log \text{PROJ}_p(\pi)(a' | s')]. \quad (9)$$

The top- $p$  operator  $\mathcal{B}_p^\pi$  is defined by projecting  $\pi$  onto  $\mathcal{A}_p^*$ . To characterize the optimality of  $\mathcal{B}_p^\pi$ , we define the supported  $q$ -norm to measure the magnitude of vectors w.r.t. the action set of interest  $\mathcal{A}_p^*$ :

**Definition 5** (supported  $q$ -norm). *For  $\Phi : \mathcal{S} \times \mathcal{Y} \rightarrow \mathbb{R}$ , we define the supported  $q$ -norm by,*

$$\|\Phi\|_{q, \mathcal{Y}} := \max_s (\sum_{a \in \mathcal{Y}} |\Phi(s, a)|^q)^{1/q}. \quad (10)$$

And slightly abusing notations, for  $\Phi : \mathcal{S} \times \mathcal{A} \rightarrow \mathbb{R}$  and  $\bar{\Phi} : \mathcal{S} \times \mathcal{A}_p^* \rightarrow \mathbb{R}$ , we define

$$\|\Phi - \bar{\Phi}\|_{q, \mathcal{A}_p^*} := \max_s (\sum_{a \in \mathcal{A}_p^*} |\Phi(s, a) - \bar{\Phi}(s, a)|^q)^{1/q}. \quad (11)$$

Note that the supported  $q$ -norm is not exactly a norm because the definiteness does not hold. However, non-negativity, homogeneity, and especially the triangle inequality do hold.

### 3.2 Optimality in $\mathcal{M}_p$

**Definition 6** (fixed point of  $\mathcal{B}_p^\pi$ ).  *$\bar{Q} : \mathcal{S} \times \mathcal{A}_p^* \rightarrow \mathbb{R}$  is a fixed point of  $\mathcal{B}_p^\pi$  iff*

$$\bar{Q}(s, a) = (\mathcal{B}_p^\pi \bar{Q})(s, a) \quad \text{for all } s \in \mathcal{S} \text{ and } a \in \mathcal{A}_p^*. \quad (12)$$

**Proposition 1** (contraction).  *$\mathcal{B}_p^\pi$  is a contraction in the supported  $\infty$ -norm.*

We start with characterizing the gap between  $\bar{Q}^{\text{PROJ}_p \pi^*}$  and  $Q^*$ , and then the characterization of  $\bar{Q}_p^*$ , the optimal value function in  $\mathcal{M}_p$ , will follow directly from the sandwich condition 3.

**Proposition 2.** *Suppose  $\kappa(p) := -\frac{\gamma}{1-\gamma} \log p$  and  $\bar{Q}^{\text{PROJ}_p \pi^*}$  is the fixed point of  $\mathcal{B}_p^{\text{PROJ}_p \pi^*}$ , the sub-optimality  $\|Q^* - \bar{Q}^{\text{PROJ}_p \pi^*}\|_{\infty, \mathcal{A}_p^*} \leq \kappa(p)$ .*

Proposition 2 shows that the sub-optimality between  $\bar{Q}^{\text{PROJ}_p \pi^*}$  and  $Q_p^*$  is bounded. This suggests that the optimal policy  $\pi^*$  in  $\mathcal{M}$  projected onto  $\mathcal{A}_p^*$ , the action set of  $\mathcal{M}_p$ , is still a good policy. While projection is trivial in the tabular case, it is in general difficult to project a parameterized  $\pi^*$  onto the action set  $\mathcal{A}_p^*$ . Instead, it is natural to implement an (inverse) RL algorithm in  $\mathcal{M}_p$ .

However, when implementing conventional IRL algorithms in  $\mathcal{M}_p$ , these algorithms typically seek to find the optimal policy  $\pi_p^*$  in  $\mathcal{M}_p$  rather than the projected  $\text{PROJ}_p \pi^*$ . The quantity of interest is the gap  $\|Q^* - \bar{Q}_p^*\|_{\infty, \mathcal{A}_p^*}$ , which measures how well  $\mathcal{M}_p$  approximates the original task  $\mathcal{M}$  using the action subset  $\mathcal{A}_p^*$ . This is intuitive: since  $\pi_p^*$  is optimal in  $\mathcal{M}_p$ , it should perform at least as well as any projected policy, including  $\text{PROJ}_p \pi^*$ .

Formally, we first provide a sandwich condition in Proposition 3, and the desired gap, as shown in Proposition 4, trivially follows.

**Proposition 3** (sandwich condition).  *$\bar{Q}^{\text{PROJ}_p \pi^*}(s, a) \leq \bar{Q}_p^*(s, a) \leq Q^*(s, a)$ , for all  $(s, a) \in \mathcal{S} \times \mathcal{A}_p^*$ .*

**Proposition 4** (bounded sub-optimality). *Given a MDP  $\mathcal{M}$  and its top- $p$  counterpart  $\mathcal{M}_p$ , let  $Q^*$  and  $\bar{Q}_p^*$  be their optimal soft  $Q$ -functions, respectively, we have:  $\|Q^* - \bar{Q}_p^*\|_{\infty, \mathcal{A}_p^*} \leq \kappa(p)$ .*

The takeaway is: **The optimal policy  $\pi_p^*$  learned in  $\mathcal{M}_p$  is provably near-optimal relative to  $\pi^*$  (the teacher), as established by Proposition 4.** This guarantee means one can deploy any IRL algorithm within  $\mathcal{M}_p$  and (theoretically) find a policy whose performance closely matches that of  $\pi^*$ , even though the action subset  $\mathcal{A}_p^*$  (for reasonable choice of  $p$ ) is much smaller than the full action space  $\mathcal{A}$ , i.e. the raw vocabulary  $\mathcal{V}$ . This makes TD learning more efficient. In the next section, we show how to tailor a concrete IRL algorithm to our top- $p$  MDP  $\mathcal{M}$ .

---

**Algorithm 1** Bellman Distill

---

**Input:** Teacher model  $\pi^*$ ; Instruction set  $\mathcal{D} = \{X\}$ ; Student model  $Q_\theta$ ; Pre-train dataset  $\mathcal{D}^{PT}$ .  
**Data Generation:** Generate the teacher dataset  $\mathcal{D}^* = \{X, Y^*\}$  using  $\pi^*$ .  
**for** each epoch **do**  
    Sample mini-batches  $\mathcal{D}_{\text{mini}}^*, \mathcal{D}_{\text{mini}}^{PT}$  from dataset  $\mathcal{D}^*, \mathcal{D}^{PT}$  respectively.  
    Compute  $\mathcal{F}_p^*$  according to Definition 7 and  $Q(s, a)$  using the student logits.  
    Compute  $\pi_Q(a | s) = \exp Q(s, a) / \sum_a \exp Q(s, a)$  and  $\text{PROJ}_p \pi_Q$  using Definition 3.  
    Compute the value function using  $V^{\text{PROJ}_p \pi_Q}(s) = \mathbb{E}_{\text{PROJ}_p \pi_Q} [Q(s, a) - \log \text{PROJ}_p \pi_Q(a | s)]$   
    Compute  $\mathcal{J}^*$  in Eq. 16 and the language modeling objective  $\mathcal{J}_{PT}$  for student model update.  
**end for**

---

## 4 Implementation

We’ve demonstrated that: Optimal policy  $\pi_p^*$  in  $\mathcal{M}_p$  yields a bounded sub-optimality 4 compared to the optimal policy  $\pi^*$  in the original problem  $\mathcal{M}$ . Technically, any soft IRL algorithm could be applied to  $\mathcal{M}_p$ , by tailoring its backup operator through top- $p$  projection (definition 3), as the example of top- $p$  soft Bellman operator (definition 4).

We choose IQL [38] as our base IRL algorithm, and show that how to practically implement its top- $p$  counterpart. Recall that the IQL objective is given by:

$$\max_Q \mathcal{J}^*(Q) := \mathbb{E}_{\rho^*} [\phi(Q(s, a) - \gamma V^{\pi_Q}(s'))] - (1 - \gamma) \mathbb{E}_{s_0} [V^{\pi_Q}(s_0)], \quad V^{\pi_Q}(s) := \log \sum_a \exp Q(s, a). \quad (13)$$

Often in (inverse) RL objectives, there are two functions  $Q$  and  $\pi$  depends on action  $a$ . Hence to constraint objective (13) (or any other objective) to the top- $p$  candidate action set  $\mathcal{A}_p^*$ , one should constraint these two functions to the candidate set.

**$Q$ -function masking.** We only need to update  $Q$ -values of interests, i.e.  $Q(s, a)$  for  $a \in \mathcal{A}_p^*$ .

**Definition 7** (top- $p$  mask). *For any  $Q : \mathcal{S} \times \mathcal{A} \rightarrow \mathbb{R}$ , we define a top- $p$  mask  $\mathcal{F}_p^* : \mathcal{S} \times \mathcal{A} \rightarrow \mathcal{S} \times \mathcal{A}$ :*

$$(\mathcal{F}_p^* Q)(s, a) := \begin{cases} Q(s, a), & \text{if } a \in \mathcal{A}_p^* \\ -\infty, & \text{otherwise} \end{cases} \quad (14)$$

Applying  $\mathcal{F}_p^*$  leads to:  $\max_Q \mathcal{J}^*(Q) := \mathbb{E}_{\rho^*} [\phi((\mathcal{F}_p^* Q)(s, a) - \gamma V^{\pi_Q}(s'))] - (1 - \gamma) \mathbb{E}_{s_0} [V^{\pi_Q}(s_0)]$ .

**Policy projection.** We are also ready to handle the policy  $\pi_Q$  through projection. By definition  $\pi_Q(a | s) = \exp Q(s, a) / \sum_a \exp Q(s, a)$ , as a result its projected counterpart is  $(\text{PROJ}_p \pi_Q) = \exp Q(s, a) / \sum_{\mathcal{A}_p^*} \exp Q(s, a)$  for  $a \in \mathcal{A}_p^*$  otherwise 0.

Applying both  $Q$ -function masking and policy projection leads to:

$$\max_Q \mathcal{J}^*(Q) := \mathbb{E}_{\rho^*} [\phi((\mathcal{F}_p^* Q)(s, a) - \gamma V^{\text{PROJ}_p \pi_Q}(s'))] - (1 - \gamma) \mathbb{E}_{s_0} [V^{\text{PROJ}_p \pi_Q}(s_0)] \quad (15)$$

**Further IQL details.**  $\phi(\cdot)$  is a reward regularizer, we follow Garg et al. [38] to use  $\chi^2$ , corresponding to  $\phi(x) = x - x^2/4\alpha$  for some coefficient  $\alpha$ . We use  $\alpha = 0.1$  for our experiments. In the IQL implementation, the second term in Eq. (13) is rewritten equivalently to a TD update through the telescopic identity [38]. This identity states: for any  $\pi$ , valid occupancy measure  $\mu$ , and value function  $V^\pi$ , we have  $\mathbb{E}_{(s,a) \sim \mu} [V^\pi(s) - \gamma \mathbb{E}_{s'} V^\pi(s')] = (1 - \gamma) \mathbb{E}_{s_0} [V^\pi(s_0)]$ .

Let  $\mu = \rho^*$  and  $\phi(x) = x - x^2/4\alpha$ , the projected IQL objective is thereby given by:

$$\max_Q \mathcal{J}^*(Q) := \mathbb{E}_{\rho^*} [\phi((\mathcal{F}_p^* Q)(s, a) - \gamma V^{\text{PROJ}_p \pi_Q}(s'))] - \mathbb{E}_{\rho^*} [V^{\text{PROJ}_p \pi_Q}(s) - \gamma \mathbb{E}_{s'} V^{\text{PROJ}_p \pi_Q}(s')] \quad (16)$$

where  $V^{\text{PROJ}_p \pi_Q}(s) = \mathbb{E}_{\text{PROJ}_p \pi_Q} [Q(s, a) - \log \text{PROJ}_p \pi_Q]$ . Note this is consistent with Eq. (13), since without projection we have  $V^{\pi_Q}(s) = \mathbb{E}_{\pi_Q} [Q(s, a) - \log \pi_Q(a | s)] = \log \sum_a \exp Q(s, a)$ .

Here the expectation w.r.t.  $\rho^*$  implies that data should be sampled from the teacher model  $\pi^*$ .

Table 1: **Main results:** The Rouge-L scores, averaged over five random seeds, of our method and baselines across model families. Parameter sizes are listed at the top of each block. Best results per block are in **bold**. \*: For GPT-2 class, the baseline results are directly duplicated from Gu et al. [19].

Method	<b>GPT-2*</b>			<b>OPT</b>			<b>Qwen-2.5</b>		
	Dolly	SelfInst	Vicuna	Dolly	SelfInst	Vicuna	Dolly	SelfInst	Vicuna
Teacher	1.5B			6.7B			3B		
	27.6	14.3	16.3	27.6	16.4	17.8	28.8	24.1	21.0
Student	120M			125M			0.5B		
SFT	23.2	9.9	14.3	23.2	9.9	14.3	24.5	16.5	17.6
KD	22.8	10.8	13.4	21.9	9.7	14.0	24.4	14.7	17.8
SeqKD	22.7	10.1	14.3	22.0	10.1	13.7	24.7	15.3	17.4
MiniLLM	24.6	13.2	<b>16.9</b>	23.8	10.2	<b>15.3</b>	26.7	19.1	20.5
BD (Ours)	<b>24.7</b>	<b>13.3</b>	16.2	<b>25.1</b>	<b>11.4</b>	14.8	<b>27.8</b>	<b>19.5</b>	<b>20.7</b>
Student	340M			350M			–		
SFT	25.5	13.0	16.0	23.6	10.6	15.5	–	–	–
KD	25.0	12.0	15.4	22.5	11.1	14.9	–	–	–
SeqKD	25.3	12.6	16.9	23.1	11.4	14.7	–	–	–
MiniLLM	25.4	<b>15.6</b>	<b>17.7</b>	24.3	11.5	17.9	–	–	–
BD (Ours)	<b>25.8</b>	15.4	16.5	<b>26.0</b>	<b>12.1</b>	<b>18.1</b>	–	–	–
Student	760M			1.3B			–		
SFT	25.4	12.4	16.1	26.0	11.4	15.6	–	–	–
KD	25.9	13.4	16.9	25.5	12.0	15.4	–	–	–
SeqKD	25.6	14.0	15.9	26.0	12.5	16.4	–	–	–
MiniLLM	<b>26.4</b>	15.9	<b>18.3</b>	26.2	13.7	<b>16.7</b>	–	–	–
BD (Ours)	26.2	<b>16.1</b>	17.3	<b>27.1</b>	<b>15.1</b>	16.3	–	–	–

In practice, we parameterize  $Q_\theta$  with  $\theta$ , the parameters of the student model, the student policy  $\pi_\theta = \exp Q_\theta(s, a) / \sum_{a \in \mathcal{A}} \exp Q_\theta(s, a)$ . Therefore, the  $Q_\theta$  values are effectively the (constant-shifted) logits of student network, hence it is sufficient to have one model to serve as both  $Q_\theta$ -function and student policy  $\pi_\theta$ .

**Further implementation details.** Following Gu et al. [19], we maximize a language modeling objective  $\mathcal{J}_{PT} = \mathbb{E}_{(s,a) \sim \mathcal{D}^{PT}} \log \pi_Q(a | s)$  to retain performance on established NLP benchmarks. We refer to Algorithm 1 and Section 2.3 of Gu et al. [19] for further details. We clip the Q values using a minimum value  $Q_{\min} = -10$  for numerical stability.

## 5 Experiments

In this section, we call our method as Bellman Distill (BD) for brevity.

### 5.1 Experiment Setup

We take instruction-following [44] as the conditional text generation task, where models are trained to generate responses according to the instructions. We fine-tune a large model on a dataset consisting of instruction-response pairs as the teacher model. Then, we compare different KD methods by evaluating the student model’s instruction-following performance.

**Model selections.** We conduct experiments using three model families: the GPT-2 family [45], the OPT family [46], and the Qwen-2.5 family [6]. For the GPT-2 family, we use the 1.5B model as the teacher and the 120M, 340M, and 760M models as students. In the OPT family, the 6.7B model

serves as the teacher, with the 125M, 350M, and 1.3B models as students. For the Qwen-2.5 family, we use the 3B model as the teacher and the 0.5B model as the student.

**Training.** We build our training dataset using databricks-dolly-15K (<https://github.com/databrickslabs/dolly/tree/master>), which contains 15,000 human-authored instruction-response pairs. To accommodate model constraints, we remove any samples that exceed the maximum context length. From the remaining data, we randomly select 500 examples for validation and 1,000 for testing, leaving around 12,500 samples for training. For the pretraining dataset  $\mathcal{D}^{PT}$ , we adopt OpenWebText [47] for models in the GPT-2 and Qwen-2.5 families, and use the RoBERTa training corpus [48] for OPT models. Following the MiniLLM setup [19], we select hyperparameters based on Rouge-L [49] scores evaluated on the validation set.

As our approach operates in an offline setting, we begin by generating responses from a teacher model using queries from dataset  $\mathcal{D}$ . Each query may yield multiple responses. These query-response pairs are then used to fine-tune the student models. Additional training details are provided in Appendix B.

**Baselines choices.** Following [19], we choose four baselines: (i) **SFT** directly fine-tunes the student model on  $\mathcal{D}$  with golden responses; (ii) **KD** [9, 50] fine-tunes the student model on  $\mathcal{D}$  using the teacher distribution as supervision at each token step, also known as word-level KD; (iii) **SeqKD** [8, 51–54] fine-tunes the student model on the response sequences generated by the teacher model; (iv) **MiniLLM** [19] fine-tunes the student model using a policy gradient approach, where the reward is defined by the reverse KL divergence between the output distributions of the teacher and student.

**Evaluation.** Following [19], we evaluate the trained models on three instruction-following datasets: (i) **DollyEval**: The 500-sample test set we split from the databricks-dolly-15K dataset; (ii) **SelfInst**: [55] A user-oriented instruction-following set with 252 samples; (iii) **Vicuna**: [51] The 80 challenging questions used in the Vicuna evaluation.

**Metrics.** Following [19], we employ two complementary evaluation metrics: (i) **Rouge-L** [49] to assess the precision of generated responses, following prior work demonstrating its effectiveness for large-scale instruction-following evaluation [56]; (ii) **Win rate** of our approach evaluated by a GPT-4o-mini [57] oracle against baseline methods to measure generation quality.

A more detailed description on data generation and evaluation can be found in Appendix C.

## 5.2 Experimental Results

We present our experimental results in terms of Rouge-L scores for the GPT-2, OPT, and Qwen-2.5 model families in Table 1. We also demonstrate the win rate results in Figure 2. Our method consistently outperforms the KD and SeqKD baselines across all settings. While our approach performs comparably to MiniLLM on the GPT-2 family, it generally surpasses MiniLLM on the OPT and Qwen-2.5 families. Furthermore, the results highlight the scalability of our method across different student model sizes within all three families: as the student model size increases, the Rouge-L score also improves. This demonstrates the strong scalability and generalization ability of our approach across both model sizes and architectures.

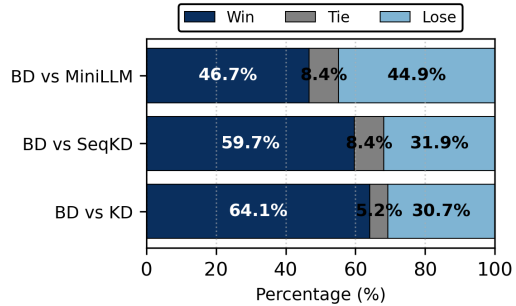


Figure 2: Comparison of win rates against KD, SeqKD, and MiniLLM baselines. We evaluate using GPT-4o-mini [57] as the judging oracle, with Qwen-2.5 (3B) as the teacher model and a smaller (0.5B) model as the student. Results are based on 500 responses per distilled model, generated under the Dolly evaluation setting.

## 5.3 Impact of $p$

In this section, we analyze the impact of the top- $p$  value in the top- $p$  distillation setting. We conduct the analysis using GPT-2 340M, OPT 125M, and Qwen-2.5 0.5B models, with results shown in Table 2 for  $p = 0.5, 0.8$ , and  $1.0$ . The table shows that omitting the top- $p$  mask (i.e., using  $p = 1.0$ ) leads to a notable drop in distillation performance. When  $p = 0.5$ , performance on OPT 125M is slightly lower than with  $p = 0.8$ , while the results are comparable for the other two models. Based



Table 2: **Impact of  $p$ :** We demonstrate the impact of different choices of  $p$  across three models from distinct model families. Results are reported using the Rouge-L score and averaged over five random seeds. The performance gains relative to the baseline ( $p = 1.0$ , without top- $p$  mask) are shown in **green**. It is evident that our top- $p$  framework achieves consistent improvements.

Models	GPT-2 1.5B $\rightarrow$ 340M			OPT 6.7B $\rightarrow$ 125M			Qwen-2.5 3B $\rightarrow$ 0.5B		
	Dolly	SelfInst	Vicuna	Dolly	SelfInst	Vicuna	Dolly	SelfInst	Vicuna
1.0	24.9	15.2	15.7	23.6	10.5	14.2	26.6	18.1	18.6
0.8	25.8(+0.9)	15.4(+0.2)	16.5(+0.8)	25.1(+1.5)	11.4(+0.9)	14.8(+0.6)	27.8(+1.2)	19.5(+1.4)	20.7(+2.1)
0.5	25.6(+0.7)	15.5(+0.3)	16.1(+0.4)	24.4(+0.8)	11.0(+0.5)	14.7(+0.5)	27.6(+1.0)	19.2(+1.1)	20.2(+1.6)

Table 3: **Training time comparison:** Our approach achieves the optimal validation performance in significantly less training time compared to Gu et al. [19], thanks to its offline training paradigm.

Models	GPT-2 1.5B $\rightarrow$ 340M	OPT 6.7B $\rightarrow$ 350M	Qwen-2.5 3B $\rightarrow$ 0.5B
MiniLLM	11.2h	12.8h	10.7h
BD (Ours)	1.3h	3.5h	0.8h

Table 4:  **$\chi^2$  regularization:** We demonstrate the effectiveness of incorporating  $\chi^2$  regularization into the distillation objective. Results reported are the Rouge-L score, averaged over five random seeds.

Models	GPT-2 1.5B $\rightarrow$ 760M			Qwen-2.5 3B $\rightarrow$ 0.5B		
	Dolly	SelfInst	Vicuna	Dolly	SelfInst	Vicuna
w $\chi^2$ regularization	26.2	16.1	17.3	27.8	19.5	20.7
w/o $\chi^2$ regularization	25.9	15.7	17.1	27.4	19.2	20.3

on this observation, we adopt  $p = 0.8$  in most experiments reported in Table 1, except when using OPT 1.3B as the student model, where  $p = 0.5$  yields slightly better results.

## 5.4 Training Time

**Online vs offline training.** In general, the choice between online and offline training is a trade-off between computational cost and performance. While auto-regressive online generation is computationally expensive, offline training allows for the reuse of pre-collected datasets, making it more efficient. However, online training typically yields better final performance [58–60, 38]. In particular, Wen et al. [20], Ko et al. [21] discussed how the offline setting can accelerate distillation, especially given the high cost of online generation for LLMs. We choose offline training due to computational constraints, although the proposed approach is inherently agnostic to the choice of training setting.

**Wall-time comparison.** To demonstrate the computational efficiency of our offline approach, we compare its training time to reach the optimal validation performance with the online method Gu et al. [19]. All experiments are conducted on 4×A40 GPUs. Results are shown in Table 3.

## 5.5 Ablation on the $\chi^2$ Regularization

We perform an ablation study on the use of  $\chi^2$  regularization, as introduced in Section , to assess its impact on distillation performance. Our empirical results show that incorporating  $\chi^2$  regularization improves the performance of the distilled student model. The study is conducted on two distillation setups: GPT-2 1.5B to 760M and Qwen-2.5 3B to 0.5B. The results are presented in Table 4.

## 6 Discussions

**Further related works.** From the imitation learning (IL) perspective, language model distillation can be viewed as a form of IL—or more broadly, reinforcement learning (RL)—in large discrete action spaces [61–65], a significant line of research in deep (inverse) RL. A common approach in this setting is to develop methods that restrict the action space to a manageable subset. This remains a

core challenge in (inverse) RL, where little prior knowledge is available about the full action space. In contrast, distillation benefits from access to a teacher model, which enables efficient identification of high-quality action subsets. This insight directly motivates our top- $p$  TD learning design.

**Limitations.** A limitation of this work—and of white-box language model distillation in general—is the requirement that the teacher and student share an identical vocabulary. This constraint arises from the need to match their output distributions, either explicitly (as in BC) or implicitly (as in IRL).

**Conclusions.** To summarize, motivated by the observation that a small number of top tokens contribute the majority of the total probability mass, we proposed a top- $p$  TD learning framework that operates over a top- $p$  candidate action subset  $\mathcal{A}_p^*$ . This framework is, in principle, plug-and-play and can be integrated into any TD-based IRL algorithm. We demonstrated its practicality through a concrete implementation of top- $p$  IQL and showed its empirical performance gains.

## References

- [1] Josh Achiam, Steven Adler, Sandhini Agarwal, Lama Ahmad, Ilge Akkaya, Florencia Leoni Aleman, Diogo Almeida, Janko Altenschmidt, Sam Altman, Shyamal Anadkat, et al. Gpt-4 technical report. *arXiv preprint arXiv:2303.08774*, 2023.
- [2] Hugo Touvron, Thibaut Lavril, Gautier Izacard, Xavier Martinet, Marie-Anne Lachaux, Timothée Lacroix, Baptiste Rozière, Naman Goyal, Eric Hambro, Faisal Azhar, et al. Llama: Open and efficient foundation language models. *arXiv preprint arXiv:2302.13971*, 2023.
- [3] Aaron Grattafiori, Abhimanyu Dubey, Abhinav Jauhri, Abhinav Pandey, Abhishek Kadian, Ahmad Al-Dahle, Aiesha Letman, Akhil Mathur, Alan Schelten, Alex Vaughan, et al. The llama 3 herd of models. *arXiv preprint arXiv:2407.21783*, 2024.
- [4] Daya Guo, Dejian Yang, Haowei Zhang, Junxiao Song, Ruoyu Zhang, Runxin Xu, Qihao Zhu, Shirong Ma, Peiyi Wang, Xiao Bi, et al. Deepseek-r1: Incentivizing reasoning capability in llms via reinforcement learning. *arXiv preprint arXiv:2501.12948*, 2025.
- [5] Jinze Bai, Shuai Bai, Yunfei Chu, Zeyu Cui, Kai Dang, Xiaodong Deng, Yang Fan, Wenbin Ge, Yu Han, Fei Huang, et al. Qwen technical report. *arXiv preprint arXiv:2309.16609*, 2023.
- [6] An Yang, Baosong Yang, Beichen Zhang, Binyuan Hui, Bo Zheng, Bowen Yu, Chengyuan Li, Dayiheng Liu, Fei Huang, Haoran Wei, et al. Qwen2. 5 technical report. *arXiv preprint arXiv:2412.15115*, 2024.
- [7] Geoffrey Hinton, Oriol Vinyals, and Jeff Dean. Distilling the knowledge in a neural network. *arXiv preprint arXiv:1503.02531*, 2015.
- [8] Yoon Kim and Alexander M Rush. Sequence-level knowledge distillation. In *Proceedings of the 2016 conference on empirical methods in natural language processing*, pages 1317–1327, 2016.
- [9] Victor Sanh, Lysandre Debut, Julien Chaumond, and Thomas Wolf. Distilbert, a distilled version of bert: smaller, faster, cheaper and lighter. *arXiv preprint arXiv:1910.01108*, 2019.
- [10] Xiaoqi Jiao, Yichun Yin, Lifeng Shang, Xin Jiang, Xiao Chen, Linlin Li, Fang Wang, and Qun Liu. Tinybert: Distilling bert for natural language understanding. *arXiv preprint arXiv:1909.10351*, 2019.
- [11] Wenhui Wang, Furu Wei, Li Dong, Hangbo Bao, Nan Yang, and Ming Zhou. Minilm: Deep self-attention distillation for task-agnostic compression of pre-trained transformers. *Advances in neural information processing systems*, 33:5776–5788, 2020.
- [12] Dean A Pomerleau. Efficient training of artificial neural networks for autonomous navigation. *Neural computation*, 3(1):88–97, 1991.
- [13] Pieter Abbeel and Andrew Y Ng. Apprenticeship learning via inverse reinforcement learning. In *Proceedings of the twenty-first international conference on Machine learning*, page 1, 2004.

- [14] Stuart Russell. Learning agents for uncertain environments. In *Proceedings of the eleventh annual conference on Computational learning theory*, pages 101–103, 1998.
- [15] Andrew Y Ng, Stuart Russell, et al. Algorithms for inverse reinforcement learning. In *Icml*, volume 1, page 2, 2000.
- [16] Brian D Ziebart, Andrew L Maas, J Andrew Bagnell, Anind K Dey, et al. Maximum entropy inverse reinforcement learning. In *Aaai*, volume 8, pages 1433–1438. Chicago, IL, USA, 2008.
- [17] Jonathan Ho and Stefano Ermon. Generative adversarial imitation learning. *Advances in neural information processing systems*, 29, 2016.
- [18] Rishabh Agarwal, Nino Vieillard, Yongchao Zhou, Piotr Stanczyk, Sabela Ramos Garea, Matthieu Geist, and Olivier Bachem. On-policy distillation of language models: Learning from self-generated mistakes. In *The Twelfth International Conference on Learning Representations*, 2024.
- [19] Yuxian Gu, Li Dong, Furu Wei, and Minlie Huang. Minillm: Knowledge distillation of large language models. *arXiv preprint arXiv:2306.08543*, 2023.
- [20] Yuqiao Wen, Zichao Li, Wenyu Du, and Lili Mou. F-divergence minimization for sequence-level knowledge distillation. *arXiv preprint arXiv:2307.15190*, 2023.
- [21] Jongwoo Ko, Sungnyun Kim, Tianyi Chen, and Se-Young Yun. Distillm: Towards streamlined distillation for large language models. *arXiv preprint arXiv:2402.03898*, 2024.
- [22] Stéphane Ross, Geoffrey Gordon, and Drew Bagnell. A reduction of imitation learning and structured prediction to no-regret online learning. In *Proceedings of the fourteenth international conference on artificial intelligence and statistics*, pages 627–635. JMLR Workshop and Conference Proceedings, 2011.
- [23] Stephen Tu, Alexander Robey, Tingnan Zhang, and Nikolai Matni. On the sample complexity of stability constrained imitation learning. In *Learning for Dynamics and Control Conference*, pages 180–191. PMLR, 2022.
- [24] Marc’Aurelio Ranzato, Sumit Chopra, Michael Auli, and Wojciech Zaremba. Sequence level training with recurrent neural networks. *arXiv preprint arXiv:1511.06732*, 2015.
- [25] Umar Syed, Michael Bowling, and Robert E Schapire. Apprenticeship learning using linear programming. In *Proceedings of the 25th international conference on Machine learning*, pages 1032–1039, 2008.
- [26] Takayuki Osa, Joni Pajarinen, Gerhard Neumann, J Andrew Bagnell, Pieter Abbeel, Jan Peters, et al. An algorithmic perspective on imitation learning. *Foundations and Trends® in Robotics*, 7(1-2):1–179, 2018.
- [27] Richard S Sutton, Andrew G Barto, et al. *Reinforcement learning: An introduction*, volume 1. MIT press Cambridge, 1998.
- [28] Lantao Yu, Weinan Zhang, Jun Wang, and Yong Yu. Seqgan: Sequence generative adversarial nets with policy gradient. In *Proceedings of the AAAI conference on artificial intelligence*, volume 31, 2017.
- [29] Qingyang Wu, Lei Li, and Zhou Yu. Textgail: Generative adversarial imitation learning for text generation. In *Proceedings of the AAAI Conference on Artificial Intelligence*, volume 35, pages 14067–14075, 2021.
- [30] Chen Jia. Adversarial moment-matching distillation of large language models. *arXiv preprint arXiv:2406.02959*, 2024.
- [31] Gokul Swamy, Sanjiban Choudhury, J Andrew Bagnell, and Steven Wu. Of moments and matching: A game-theoretic framework for closing the imitation gap. In *International Conference on Machine Learning*, pages 10022–10032. PMLR, 2021.

- [32] Charlie Snell, Ilya Kostrikov, Yi Su, Mengjiao Yang, and Sergey Levine. Offline rl for natural language generation with implicit language q learning. *arXiv preprint arXiv:2206.11871*, 2022.
- [33] Zishun Yu, Yunzhe Tao, Liyu Chen, Tao Sun, and Hongxia Yang.  $\beta$ -coder: Value-based deep reinforcement learning for program synthesis. *arXiv preprint arXiv:2310.03173*, 2023.
- [34] Alexander Havrilla, Maksym Zhuravinskyi, Duy Phung, Aman Tiwari, Jonathan Tow, Stella Biderman, Quentin Anthony, and Louis Castricato. trlx: A framework for large scale reinforcement learning from human feedback. In *Proceedings of the 2023 Conference on Empirical Methods in Natural Language Processing*, pages 8578–8595, 2023.
- [35] Michael Lederman Littman. *Algorithms for sequential decision-making*. Brown University, 1996.
- [36] Tuomas Haarnoja, Aurick Zhou, Pieter Abbeel, and Sergey Levine. Soft actor-critic: Off-policy maximum entropy deep reinforcement learning with a stochastic actor. In *International conference on machine learning*, pages 1861–1870. Pmlr, 2018.
- [37] Stefan Banach. Sur les opérations dans les ensembles abstraits et leur application aux équations intégrales. *Fundamenta mathematicae*, 3(1):133–181, 1922.
- [38] Divyansh Garg, Shuvam Chakraborty, Chris Cundy, Jiaming Song, and Stefano Ermon. Iq-learn: Inverse soft-q learning for imitation. *Advances in Neural Information Processing Systems*, 34: 4028–4039, 2021.
- [39] John M Danskin. *The theory of max-min and its application to weapons allocation problems*, volume 5. Springer Science & Business Media, 2012.
- [40] Firas Al-Hafez, Davide Tateo, Oleg Arenz, Guoping Zhao, and Jan Peters. Ls-iq: Implicit reward regularization for inverse reinforcement learning. *arXiv preprint arXiv:2303.00599*, 2023.
- [41] Kavosh Asadi and Michael L Littman. An alternative softmax operator for reinforcement learning. In *International Conference on Machine Learning*, pages 243–252. PMLR, 2017.
- [42] Erfan Miah, Revan MacQueen, Alex Ayoub, Abbas Masoumzadeh, and Martha White. Resmax: An alternative soft-greedy operator for reinforcement learning. *Transactions on Machine Learning Research*.
- [43] Ari Holtzman, Jan Buys, Li Du, Maxwell Forbes, and Yejin Choi. The curious case of neural text degeneration. *arXiv preprint arXiv:1904.09751*, 2019.
- [44] Long Ouyang, Jeffrey Wu, Xu Jiang, Diogo Almeida, Carroll Wainwright, Pamela Mishkin, Chong Zhang, Sandhini Agarwal, Katarina Slama, Alex Ray, et al. Training language models to follow instructions with human feedback. *Advances in neural information processing systems*, 35:27730–27744, 2022.
- [45] Alec Radford, Jeff Wu, Rewon Child, David Luan, Dario Amodei, and Ilya Sutskever. Language models are unsupervised multitask learners. 2019.
- [46] Susan Zhang, Stephen Roller, Naman Goyal, Mikel Artetxe, Moya Chen, Shuohui Chen, Christopher Dewan, Mona Diab, Xian Li, Xi Victoria Lin, et al. Opt: Open pre-trained transformer language models. *arXiv preprint arXiv:2205.01068*, 2022.
- [47] Aaron Gokaslan and Vanya Cohen. Openwebtext corpus. <http://Skylion007.github.io/OpenWebTextCorpus>, 2019.
- [48] Yinhan Liu, Myle Ott, Naman Goyal, Jingfei Du, Mandar Joshi, Danqi Chen, Omer Levy, Mike Lewis, Luke Zettlemoyer, and Veselin Stoyanov. Roberta: A robustly optimized bert pretraining approach. *arXiv preprint arXiv:1907.11692*, 2019.
- [49] Chin-Yew Lin. ROUGE: A package for automatic evaluation of summaries. In *Text Summarization Branches Out*, pages 74–81, Barcelona, Spain, July 2004. Association for Computational Linguistics. URL <https://aclanthology.org/W04-1013/>.

- [50] Kaitao Song, Hao Sun, Xu Tan, Tao Qin, Jianfeng Lu, Hongzhi Liu, and Tie-Yan Liu. Lightpaff: A two-stage distillation framework for pre-training and fine-tuning. *arXiv preprint arXiv:2004.12817*, 2020.
- [51] Wei-Lin Chiang, Zhuohan Li, Zi Lin, Ying Sheng, Zhanghao Wu, Hao Zhang, Lianmin Zheng, Siyuan Zhuang, Yonghao Zhuang, Joseph E. Gonzalez, Ion Stoica, and Eric P. Xing. Vicuna: An open-source chatbot impressing gpt-4 with 90%\* chatgpt quality, March 2023. URL <https://lmsys.org/blog/2023-03-30-vicuna/>.
- [52] Rohan Taori, Ishaan Gulrajani, Tianyi Zhang, Yann Dubois, Xuechen Li, Carlos Guestrin, Percy Liang, and Tatsunori B. Hashimoto. Stanford alpaca: An instruction-following llama model. [https://github.com/tatsu-lab/stanford\\_alpaca](https://github.com/tatsu-lab/stanford_alpaca), 2023.
- [53] Baolin Peng, Chunyuan Li, Pengcheng He, Michel Galley, and Jianfeng Gao. Instruction tuning with gpt-4. *arXiv preprint arXiv:2304.03277*, 2023.
- [54] Chunting Zhou, Pengfei Liu, Puxin Xu, Srinivasan Iyer, Jiao Sun, Yuning Mao, Xuezhe Ma, Avia Efrat, Ping Yu, Lili Yu, et al. Lima: Less is more for alignment. *Advances in Neural Information Processing Systems*, 36:55006–55021, 2023.
- [55] Yizhong Wang, Yeganeh Kordi, Swaroop Mishra, Alisa Liu, Noah A Smith, Daniel Khoshdel, and Hannaneh Hajishirzi. Self-instruct: Aligning language models with self-generated instructions. *arXiv preprint arXiv:2212.10560*, 2022.
- [56] Yizhong Wang, Swaroop Mishra, Pegah Alipoormolabashi, Yeganeh Kordi, Amirreza Mirzaei, Anjana Arunkumar, Arjun Ashok, Arut Selvan Dhanasekaran, Atharva Naik, David Stap, et al. Super-naturalinstructions: Generalization via declarative instructions on 1600+ nlp tasks. *arXiv preprint arXiv:2204.07705*, 2022.
- [57] OpenAI. Gpt-4o mini: advancing cost-efficient intelligence, 2024. URL <https://openai.com/index/gpt-4o-mini-advancing-cost-efficient-intelligence/>.
- [58] Edouard Klein, Matthieu Geist, and Olivier Pietquin. Batch, off-policy and model-free apprenticeship learning. In *European Workshop on Reinforcement Learning*, pages 285–296. Springer, 2011.
- [59] Donghun Lee, Srivatsan Srinivasan, and Finale Doshi-Velez. Truly batch apprenticeship learning with deep successor features. *arXiv preprint arXiv:1903.10077*, 2019.
- [60] Daniel Jarrett, Ioana Bica, and Mihaela van der Schaar. Strictly batch imitation learning by energy-based distribution matching. *Advances in Neural Information Processing Systems*, 33: 7354–7365, 2020.
- [61] Gabriel Dulac-Arnold, Richard Evans, Hado van Hasselt, Peter Sunehag, Timothy Lillicrap, Jonathan Hunt, Timothy Mann, Theophane Weber, Thomas Degris, and Ben Coppin. Deep reinforcement learning in large discrete action spaces. *arXiv preprint arXiv:1512.07679*, 2015.
- [62] Chen Tessler, Tom Zahavy, Deborah Cohen, Daniel J Mankowitz, and Shie Mannor. Action assembly: Sparse imitation learning for text based games with combinatorial action spaces. *arXiv preprint arXiv:1905.09700*, 2019.
- [63] Fabian Akkerman, Julius Luy, Wouter van Heeswijk, and Maximilian Schiffer. Dynamic neighborhood construction for structured large discrete action spaces. *arXiv preprint arXiv:2305.19891*, 2023.
- [64] Yuta Saito, Qingyang Ren, and Thorsten Joachims. Off-policy evaluation for large action spaces via conjunct effect modeling. In *international conference on Machine learning*, pages 29734–29759. PMLR, 2023.
- [65] Fares Fourati, Vaneet Aggarwal, and Mohamed-Slim Alouini. Stochastic q-learning for large discrete action spaces. *arXiv preprint arXiv:2405.10310*, 2024.

## A Omitted Proofs

### A.1 Proposition 1

*Proof.* For any  $\bar{Q} : \mathcal{S} \times \mathcal{A}_p^* \rightarrow \mathbb{R}$  and any policy  $\pi : \mathcal{S} \rightarrow \Delta(\mathcal{A})$

$$\|\mathcal{B}_p^\pi \bar{Q}_1 - \mathcal{B}_p^\pi \bar{Q}_2\|_{\infty, \mathcal{A}_p^*}$$

by definition of supported  $\infty$  norm and  $\mathcal{B}_p^\pi$ , and  $r(s, a)$  cancels,

$$\begin{aligned} &\leq \max_{s, a} \gamma |\mathbb{E}_{a' \sim \text{PROJ}_p(\pi)} [\bar{Q}_1(s', a') - \log \text{PROJ}_p(\pi)(a'|s')] - \mathbb{E}_{a' \sim \text{PROJ}_p(\pi)} [\bar{Q}_2(s', a') - \log \text{PROJ}_p(\pi)(a'|s')]| \\ &= \max_{s, a} \gamma |\mathbb{E}_{a' \sim \text{PROJ}_p(\pi)} [\bar{Q}_1(s', a')] - \mathbb{E}_{a' \sim \text{PROJ}_p(\pi)} [\bar{Q}_2(s', a')]| \\ &\leq \gamma \max_{s'} \max_{a' \in \mathcal{A}_p^*} |\bar{Q}_1(s', a') - \bar{Q}_2(s', a')| =: \|\bar{Q}_1 - \bar{Q}_2\|_{\infty, \mathcal{A}_p^*} \end{aligned}$$

Hence  $\mathcal{B}_p^\pi$  is contraction in  $\|\cdot\|_{\infty, \mathcal{A}_p^*}$ .  $\square$

### A.2 Proposition 2

*Proof.* For brevity, we drop the norm subscripts  $\infty$  and  $\mathcal{A}_p^*$ , and we use  $\hat{Q}_p^*$  and  $\hat{\mathcal{B}}_p^*$  to denote  $\bar{Q}^{\text{PROJ}_p \pi^*}$  and  $\mathcal{B}_p^{\text{PROJ}_p \pi^*}$ , respectively.

$$\underbrace{\|Q^* - \hat{Q}_p^*\|_{\infty, \mathcal{A}_p^*}}_{=: \delta} = \|\mathcal{B}^* Q^* - \hat{\mathcal{B}}_p^* \hat{Q}_p^*\| \leq \|\hat{\mathcal{B}}_p^* Q^* - \hat{\mathcal{B}}_p^* \hat{Q}_p^*\| + \|\mathcal{B}^* Q^* - \hat{\mathcal{B}}_p^* Q^*\|$$

since  $\hat{\mathcal{B}}_p^*$  is a contractor,

$$\begin{aligned} &\leq \gamma \delta + \gamma \max_{s, a \in \mathcal{A}_p^*} |\mathbb{E}_{\pi^*} [(Q^* - \log \pi^*)(y|x)] - \mathbb{E}_{\text{PROJ}_p \pi^*} [(Q^* - \log \text{PROJ}_p \pi^*)(y|x)]| \\ &= \gamma \delta + \gamma \max_{s, a \in \mathcal{A}_p^*} \left| \sum_{y \in \mathcal{A}} \pi^*(y|x) (Q^* - \log \pi^*)(y|x) - \sum_{y \in \mathcal{A}_p^*} \frac{1}{p} \pi^*(y|x) \left( Q^* - \log \frac{1}{p} \pi^* \right) (y|x) \right| \\ &= \gamma \delta + \gamma \max_{s, a \in \mathcal{A}_p^*} \left| \sum_{y \in \mathcal{A}} \pi^*(y|x) (Q^* - \log \pi^*)(y|x) - \frac{1}{p} \sum_{y \in \mathcal{A}_p^*} \pi^*(y|x) (Q^* - \log \pi^*)(y|x) - \log p \right| \end{aligned}$$

given  $\pi^*(a|s) = \exp Q^*(s, a) / Z(s)$ , where  $Z(s) := \sum_{\mathcal{A}} \exp Q^*(s, a)$ .

$$= \gamma \delta + \gamma \max_{s, a \in \mathcal{A}_p^*} \left| \sum_{y \in \mathcal{A}} \pi^*(y|x) \log Z(x) - \frac{1}{p} \sum_{y \in \mathcal{A}_p^*} \pi^*(y|x) \log Z(x) - \log p \right|$$

since  $\sum_{y \in \mathcal{A}_p^*} \pi(y|x) = p$

$$= \gamma \delta - \gamma \log p$$

Rearranging concludes the proof.  $\square$

### A.3 Proposition 3

*Proof.* (i)  $Q^*(s, a) \geq \bar{Q}_p^*(s, a)$  follows trivially from the fact that  $Q^*$  is the optimal value function of  $\mathcal{M}$ . By definition,  $Q^*(s, a) \geq Q^\pi(s, a)$  for all  $s \in \mathcal{S}, a \in \mathcal{A}$ .

Hence  $Q^*(s, a) \geq Q^{\pi_p^*}(s, a) =: \bar{Q}^*(s, a)$  holds for all  $s \in \mathcal{S}, a \in \mathcal{A}_p^*$  as  $\mathcal{A}_p^* \subseteq \mathcal{A}$ ;

(ii) Similarly,  $\bar{Q}_p^*$  is the optimal soft  $Q$ -function in  $\mathcal{M}_p$ . We have  $\bar{Q}_p^*(s, a) \geq \bar{Q}_p^\pi(s, a)$  for all  $s \in \mathcal{S}, a \in \mathcal{A}_p^*$ . This holds for  $\text{PROJ}_p \pi$  as well, thereby  $\bar{Q}^*(s, a) \geq \bar{Q}^{\text{PROJ}_p \pi^*}(s, a)$  for all  $s \in \mathcal{S}, a \in \mathcal{A}_p^*$ .

(i) and (ii) conclude the proof.  $\square$

#### A.4 Proposition 4

*Proof.* Immediately follows from Proposition 2 and the sandwich condition Proposition 3.  $\square$

## B Training Details

Across all settings, our BD distillation process uses a batch size of 64 and a learning rate of 5e-6. We set  $p = 0.8$  for all experiments, except for the OPT 6.7B to 1.3B distillation, where we use  $p = 0.5$ . We use the regularization strength  $\alpha = 0.1$  and the discount factor  $\gamma = 0.99$  for all settings. Following the setup of Gu et al. [19], we also adopt a two-phase training strategy for our approach:

- **Phase 1:** We fine-tune the student model on the instruction-response training set  $\mathcal{D}$  to obtain a strong initialization for subsequent offline BD training. This fine-tuning is performed for 3 epochs using the optimal learning rate and batch size from the corresponding SFT baselines. Note that, unlike the SFT baseline, we select the checkpoint with the lowest validation loss during this phase, rather than the one with the highest Rouge-L score.
- **Phase 2:** We then further fine-tune the initialized student model using our distillation algorithm 0 on the teacher-generated dataset  $\mathcal{D}^*$ . The student model is trained for 3 epochs, and we select the checkpoint with the best validation Rouge-L score. All experiments are conducted on a machine with  $4 \times$  A40 GPUs.

## C Data Generation and Evaluation Details

During data generation and evaluation, we sample from each model using a temperature of 1, conditioned on a given query from the corresponding dataset. For evaluation, we use five random seeds—[10, 20, 30, 40, 50]—to perform sampling. During data generation, we sample 8 responses from the teacher model for each query in the prompt dataset to construct the teacher offline dataset  $\mathcal{D}_T$ . To convert instruction-response pairs into complete sentences, we apply the prompt wrapper shown in Figure 3.

```
Below is an instruction that describes a task.
Write a response that appropriately completes the request.

### Instruction:
{instruction}

### Input:
{input}

### Response:
{response}
```

Figure 3: Prompt wrapper for evaluation and data generation.

For the win rate evaluation, we use the prompt wrapper shown in Figure 4 to format the instruction along with one response from our method and one from a baseline method into a single sentence, which is then evaluated by the GPT-4o-mini [57] oracle. To mitigate potential bias from the ordering of options, we conduct each comparison twice—once with our method as option A and the baseline as option B, and once with the roles reversed. We then average the win rates from both evaluations.

## D Generated Examples

We present several instruction-following examples in the Vicuna setting for the distilled Qwen-2.5 model using our approach. These examples are shown in Table 5.

```

You are an impartial evaluator.
Given a question instruction, optional input context, and two
candidate answers (A and B), decide which answer is better or if they
tie. Respond with exactly one token: A, B, or Tie.

### QUESTION INSTRUCTION:
{instruction}

### ADDITIONAL CONTEXT:
{input}

### ANSWER A:
{response A}

### ANSWER B:
{response B}

Which answer is better?

```

Figure 4: Prompt wrapper for win rate evaluation using GPT-4o-mini [57].

Table 5: Examples of instruction-following responses from a distilled Qwen-2.5 0.5B model using our distillation approach.

Instruction	Generated Response
How can you determine if a restaurant is popular among locals or mainly attracts tourists, and why might this information be useful? (category: <i>common-sense</i> )	There are several metrics you can look at to determine how popular a restaurant is. One metric is the number of reviews and the type of review (in print or digital) and length of the reviews. You can look at these to see what type of reviews are coming from local residents versus tourists. There are also metrics to look at from a business perspective like average waiting time, and availability of menu changes. All of these can be useful to understand how popular a restaurant is and why that information is important.
What are the primary factors that influence consumer behavior? (category: <i>generic</i> )	There are many factors that influence consumer behavior. These include: <ul style="list-style-type: none"> <li>- Economic factors such as income, savings and budget</li> <li>- Social factors such as values, culture and fashion</li> <li>- Psychological factors such as mood and emotion</li> <li>- Consumer preferences and trends.</li> </ul>
In a world where automation is becoming increasingly prevalent, is it more important to prioritize job creation or technological progress? (category: <i>common-sense</i> )	In a world where job creation is becoming increasingly difficult to do, prioritizing technological progress is more important. Automation is a tool that can be used to help create new jobs, but it is also a tool that can be use to replace jobs that are currently existent.